COMPUTER METHODS AND PROGRAMS IN BIOMEDICINE 136 (2016) 163–177

journal homepage: www.intl.elsevierhealth.com/journals/cmpb

Cardiac arrhythmia beat classification using DOST and PSO tuned SVM

Sandeep Raj [a,*], *Kailash Chandra Ray* [a], *Om Shankar* [b]

[a] *Department of Electrical Engineering, Indian Institute of Technology Patna, Bihta, Patna 801103, India*
[b] *Department of Cardiology, Institute of Medical Sciences, Banaras Hindu University, Varanasi 221005, India*

ARTICLE INFO

Article history:
Received 13 April 2016
Received in revised form
17 August 2016
Accepted 23 August 2016

Keywords:
Cardiac arrhythmia beat
DOST
PCA
SVM
PSO

ABSTRACT

Background and objective: The increase in the number of deaths due to cardiovascular diseases (CVDs) has gained significant attention from the study of electrocardiogram (ECG) signals. These ECG signals are studied by the experienced cardiologist for accurate and proper diagnosis, but it becomes difficult and time-consuming for long-term recordings. Various signal processing techniques are studied to analyze the ECG signal, but they bear limitations due to the non-stationary behavior of ECG signals. Hence, this study aims to improve the classification accuracy rate and provide an automated diagnostic solution for the detection of cardiac arrhythmias.

Methods: The proposed methodology consists of four stages, i.e. filtering, R-peak detection, feature extraction and classification stages. In this study, Wavelet based approach is used to filter the raw ECG signal, whereas Pan–Tompkins algorithm is used for detecting the R-peak inside the ECG signal. In the feature extraction stage, discrete orthogonal Stockwell transform (DOST) approach is presented for an efficient time-frequency representation (i.e. morphological descriptors) of a time domain signal and retains the absolute phase information to distinguish the various non-stationary behavior ECG signals. Moreover, these morphological descriptors are further reduced in lower dimensional space by using principal component analysis and combined with the dynamic features (i.e based on RR-interval of the ECG signals) of the input signal. This combination of two different kinds of descriptors represents each feature set of an input signal that is utilized for classification into subsequent categories by employing PSO tuned support vector machines (SVM).

Results: The proposed methodology is validated on the baseline MIT-BIH arrhythmia database and evaluated under two assessment schemes, yielding an improved overall accuracy of 99.18% for sixteen classes in the category-based and 89.10% for five classes (mapped according to AAMI standard) in the patient-based assessment scheme respectively to the state-of-art diagnosis. The results reported are further compared to the existing methodologies in literature.

Conclusions: The proposed feature representation of cardiac signals based on symmetrical features along with PSO based optimization technique for the SVM classifier reported an improved classification accuracy in both the assessment schemes evaluated on the benchmark MIT-BIH arrhythmia database and hence can be utilized for automated computer-aided diagnosis of cardiac arrhythmia beats.

* *Corresponding author.* Department of Electrical Engineering, Indian Institute of Technology Patna, Bihta 801103, India. Fax: +91 612 3028123.
E-mail addresses: srp@iitp.ac.in (S. Raj), kcr@iitp.ac.in (K. Chandra Ray), om.shankar11@yahoo.com (O. Shankar).

http://dx.doi.org/10.1016/j.cmpb.2016.08.016
0169-2607/

1. Introduction

As per the report of the world health organization, cardiovascular diseases (CVDs) are the leading cause of mortality in the world and will remain till 2030 [1]. An estimated 17.5 million people die each year from CVDs which is a total of 31% of all deaths worldwide. Out of these more than 75% of CVD deaths occur in low-income and middle-income countries. Almost 80% of all CVD deaths are caused due to heart attacks and strokes. However, these diseases are caused due to the long-term effect of the cardiac arrhythmias occurring inside the heart that needs to be detected on time for proper diagnosis.

Electrocardiography (ECG) is a commonly utilized non-invasive diagnostic tool in clinical cardiology for analyzing long-term ECG recordings for decades. The advancement in the analysis of ECG has reported significant improvement in better management and timely diagnosis of life-threatening cardiac arrhythmias. In fact, event-by-event analysis performed by a cardiologist for the diagnosis can be tedious and time-consuming. Rather, a computer-aided automated diagnosis of cardiac signals is required, which can assist doctors to provide the medical intervention required to the patients. Therefore, automatic detection and classification of cardiac signals using different signal processing techniques [2] has evolved as an active area of research which is focused in this article. A few of these techniques include time domain analysis [3–6], statistical approach [7–9], hybrid features [10], frequency based analysis [11,12], and time-frequency analysis [13–15] for feature extraction of ECG signals. These features contain a significant amount of information about the status of the heart. These feature extraction methods are combined with the existing classifiers such as linear discriminants (LDs) [3,5,16], neural networks [12,13,17], neuro-fuzzy aproach [18] and support vector machines [19–21] for an efficient classification of cardiac abnormalities, which may not be detected with ease.

In the feature extraction stage, the statistical techniques such as PCA and ICA are nonlinear methods that are computationally complex and do not include the symmetry and reflection properties. Also, these non-linear methods do not follow the principle of superposition; hence, additivity and homogeneity principles are not followed by these methods [15]. In the transform approach, the Fourier transform fails to provide any information regarding the time of occurrence of frequency components and hence is unable to analyze the non-stationary nature of ECG signals. The ambiguities of Fourier transform is overcome by short-time Fourier transform (STFT) which provides a constant window [22]. However, the selection of the size of the window in STFT remains a challenge. This drawback of fixed window length in STFT for all frequencies is addressed by the wavelet transform (WT) [23]. The WT uses longer windows at low frequencies and shorter windows at high frequencies for the analysis of non-stationary signals. However, the proper selection of mother wavelet and sampling frequency are major factors for extracting the frequency components, failing which may result in misleading information. In fact, stockwell transform (S-transform) [22,23] overcome the drawback of WT by uniquely combining a frequency dependent resolution of time-frequency space and absolutely referenced phase information of the input signal. The S-transform localizes the real and imaginary spectra to estimate the local amplitude and phase spectrum [22,23]. The multiresolution decomposition of stockwell transform is useful but corresponds to the redundant representation of the time-frequency plane and hence is computationally expensive. Rather, a discrete and non-redundant version of the S-transform, i.e. discrete orthogonal stockwell transform (DOST) [22,23] has made the use of the S-transform more feasible. It is represented as an orthogonal set of basis functions [22,23] that localizes the spectrum and retains the advantageous properties of ST.

This article presents an efficient representation of cardiac signals in time-frequency space using discrete orthogonal stockwell transform (DOST) approach. The dimensionality of the DOST features is further reduced by employing principal component analysis (PCA). Apart from these morphological features (i.e. in the form of PCs), dynamic features are concatenated to the feature set to improve classification performance. Further, this mixture of features is utilized for classification using support vector machines. The performance parameters of the SVM classifier (i.e. the regularization and kernel parameters) are optimized using particle swarm optimization (PSO) to yield maximum performance. The PSO exploits the classifier properties in terms of the number of support vectors (SVs) and provides the best solution to the model selection issue. The proposed methodology is validated on the benchmark MIT-BIH arrhythmia database [24] and evaluated under two assessment schemes, i.e. "category-based" and "patient-based" assessment schemes. However, "category-based" assessment scheme yields promising results, but does not provide a realistic performance due to the fact that the training dataset contain similar ECG beat taken from the same patient. Therefore, "patient-based" assessment scheme is presented which predicts the record from an unseen patient (not included in the training set) to provide a realistic measure to the proposed methodology for real-time applications.

The rest of the paper is organized as follows: Section II presents the database and the assessment schemes for the implementation of the proposed methodology. Section III describes the proposed methodology while Section IV describes the results and discussion. Finally, Section V presents conclusion.

2. Database and assessment scheme

The experiments are evaluated and validated on the benchmark MIT-BIH Arrhythmia database [24]. The MIT-BIH database contains two channel ambulatory ECG recordings of 47 different patients comprising 48 records studied during 1975 and 1979 by the Beth Israel Hospital (BIH) Arrhythmia laboratory. The heartbeats in lead A signal has more prominent peaks than the lead B signal which is utilized in this study [25]. A modified limb lead II (MLII) is the lead A signal in 45 recordings, whereas V5 is the lead A signal in the other three excerpts. The database includes 110109 beat labels while the data is bandpass filtered at 0.1H-100 Hz. The excerpts are digitized with a sampling frequency of 360 samples/s and acquired with 11-bit resolution over 10 mV range. For the evaluation of the proposed

Table 1 – Training and testing datasets taken from MIT-BIH arrhythmia database.

ECG signal type—annotation	Total	Training	Testing
Normal (NOR)—N	75017	11253	63764
Left bundle branch block (LBBB)—L	8072	2825	5247
Right bundle branch block (RBBB)—R	7255	2539	4716
Atrial premature contraction (APC)—A	2546	891	1655
Preventricular contraction (PVC)—V	7129	2495	4634
Paced beat (PACE)—P	7024	2458	4566
Aberrated atrial premature beat (AP)—a	150	75	75
Ventricular flutter (VF) - !	472	236	236
Fusion of ventricular and normal beat (VFN)—F	802	401	401
Blocked atrial premature beat (BAP)—x	193	97	96
Nodal (junctional escape beat)—j	229	115	114
Fusion of paced and normal beat (FPN)—f	982	491	491
Ventricular escape beat (VE)—E	106	53	53
Nodal (junctional) premature beat (NP)—J	83	42	41
Atrial escape beat (AE)—e	16	8	8
Unclassificable beat (UN)—Q	33	17	16
Total	110,109	23,996	86,113

methodology, class annotations are used as ground truth. The experiments are performed on all the 48 records of the database and heartbeat segments are obtained using a window across each R-peak. In the "category-based" assessment scheme, a certain number of heartbeats from each of the sixteen classes are selected randomly and divided into sixteen clusters (where each cluster represents their category) from the whole dataset to constitute the training and testing datasets which is summarized in Table 1. It is to note that if there is any change in the number of cardiac beats in the training and testing datasets, the classification performance, i.e. accuracy, will also change.

Additionally, "patient-based" assessment is performed to provide a more generalized capability and realistic measure to the proposed methodology. In this assessment scheme, the database is projected into the five-classes as per the recommendations given by ANSI/AAMI EC57:1998 standard [26]. According to this standard [26], the four paced records (i.e., the records 102, 104, 107, and 217) are not included in the dataset, i.e the experiments are performed on the remaining 44 records that are equally split into the training and testing datasets each consisting of 22 records for presenting direct comparison with [3,5,16]. The sixteen classes of cardiac signals from the MIT-BIH arrhythmia database are re-splitted into the larger five categories, namely "N" (i.e., excluding the beats of S, V, F, or Q classes), "S" (i.e., supraventricular ectopic beat), "V" (i.e., ventricular ectopic beat), "F" (i.e., fusion beat), and "Q" (i.e., unknown beat) which is presented in Table 2. Additionally, the dataset containing 44 records are split into 44 folds to perform patient-by-patient (record) cross-validation featuring the cardiac signals from each patient. Thereby, to estimate the classification performance of cardiac event from a given fold, the classifier is trained on the rest of 43 folds and the procedure is repeated for all the 44 folds.

Table 2 – Mapping of MIT-BIH cardiac signal classes to AAMI signal classes.

AAMI classes	MIT-BIH classes	Total #
N	NOR, LBBB, RBBB, AE, NE	90,083
S	APC, AP, BAP, NP	2972
V	PVC, VE, VF	7480
F	VFN	802
Q	FPN, UN	15

3. Background

This section briefly describes the algorithms utilized for feature extraction, classification and optimization techniques for cardiac signal analysis which is utilized in this study.

3.1. *Discrete orthogonal stockwell transform (DOST)*

For an input signal $a(t)$, the continuous S-transform is defined as the product of Fourier transform (FT) of input signal $a(t)$ and the Gaussian window is represented as:

$$S(\tau, f) = \frac{|f|}{2\pi} \int_{-\infty}^{\infty} a(t) e^{-\frac{(t-\tau)^2 f^2}{2}} e^{-i2\pi ft} dt \quad (1)$$

where the width of the Gaussian window is given by:

$$\sigma(f) = T = \frac{1}{|f|} \quad (2)$$

In the discrete case, the S-transform is the projection of the vector defined by the time series $a[kT]$ onto a spanning set of vectors. However, the discrete versions of the ST suffer from the high redundancy, which led to the development of a transform, i.e. DOST. The DOST is an efficient representation (i.e signal of length N is transformed into N data points) with an orthogonal set of basis functions that localizes the spectrum and retains the advantageous phase properties. An orthogonal transformation takes an N-point input time series to an N-point time-frequency representation where the transformation matrix is orthogonal and each point in the representation is linearly independent from any other point. The transform samples the signal of lower frequency at a lower rate and higher frequencies at higher rate. A transform $S(\tau, f_0)$ for a constant frequency f_0 can be understood as a one-dimensional function which signifies the change in amplitude and phase of this frequency changes over time. The phase is the characteristic feature of S-transform which makes it different from wavelet of filter bank approach. The DOST transform is localized in space and reduces the time-locality. However, it contains both the frequencies, i.e. positive and negative. The time-series representation can be recovered by applying inverse DFT of this spectrum. The use of fast-Fourier transform (FFT) in factoring DOST allows to achieve $O(NlogN)$ running time complexity.

Thus, DOST representation can be defined as the inner products between a time series $h[kT]$ and the basis functions defined as a function of $[kT]$, with the parameters ν (a frequency variable indicative of the center of a frequency band), β (indicating the frequency resolution), and τ (a time variable indicating the time localization) [23].

$$S\{h[kT]\} = S\left(\tau T, \frac{\nu}{NT}\right) = \sum_{k=0}^{N-1} h[kT] S_{[\nu,\beta,\tau]}[kT] \tag{3}$$

$$S_{[\nu,\beta,\tau]}[kT] = \frac{ie^{-i\pi\tau}}{\sqrt{\beta}} \frac{e^{i2\pi\left(\frac{k}{N}-\frac{\tau}{\beta}\right)\left(\nu-\frac{\beta}{2}-\frac{1}{2}\right)} - e^{-2\pi\left(\frac{k}{N}-\frac{\tau}{\beta}\right)\left(\nu+\frac{\beta}{2}-\frac{1}{2}\right)}}{2\sin\left[\pi\left(\frac{k}{N}-\frac{\tau}{\beta}\right)\right]} \tag{4}$$

However, this expression does not account for the sampling of time-frequency space. A set of rules are followed to ensure orthogonality that samples the time-frequency space:

Rule 1. $\tau = 0, 1, \cdots, \beta - 1$.
Rule 2. The selection of ν and β such that each fourier frequency sample is used only once.

There are one or more local time samples (τ) for each frequency bandwidth which should be equal to β (as per Rule 1), also the wider the frequency resolution (large β), the greater the time resolution (large τ) [23]. Octave sampling [23] is applied to the input signal which doubles the bandwidth each increasing bandwidth. A set of specific rules on the basis functions are followed, which implies a strict definition for ν and β for partitioning the input signal.

3.2. Support vector machines

In this study, a support vector machine is employed for heartbeats classification into one of the 16 classes in the category based assessment scheme or the 5 classes in the patient based assessment scheme. SVMs are supervised learning models for solving pattern classification problems that can handle very large feature spaces. An SVM constructs a hyperplane or a set of hyperplanes in a high- or infinite-dimensional space, which is being used for classification, regression, or other tasks. SVM assumes that the data to be analyzed are linearly separable while the classes are assumed as {–1,+1}. A hyperplane is constructed by the equation $w^T x + b = 0$ (where "w" is the vector of hyperplane coefficients, "b" is a bias term) to maximize the margin between the hyperplane and the support vectors (nearest data points). The optimal hyperplane constructed minimizes a cost function based on two criteria, i.e. margin maximization and error minimization and represented as $\phi(w, \xi) = \frac{1}{2}\|w\|^2 + c\sum_{i=1}^{N} \xi_i$ where "C" is a value which determines the trade-off between model complexity $\|w\|^2$ and minimizing training errors. The minimization issue is referred to as the quadratic optimization (QP) problem. The solution results in the decision function of the form $f(x) = sgn\left[\sum_{i=1}^{N} y_i \alpha_i (x.x_i) b\right]$. The feasibility of quadratic complexity is only for low-dimensional data and involves a huge memory and consumption of time for processing.

Originally SVMs classify the data in linear case, while in the non-linear case SVMs do not achieve the classification tasks. This limitation can be overcome by a kernel based approach which performs a non-linear classification and implicitly maps the inputs into high-dimensional feature spaces. The idea beside the kernel function is to enable operations to be performed in the input space rather than the potentially high dimensional feature space. SVMs were originally designed for binary classification. To overcome this ambiguity, several approaches are proposed to extend SVM for multi-class classification which includes (i) one-against-one (ONO) and (ii) one-against-all (OAA).

In this study, one-against-one approach (OAO) is utilized that generates $N(N-1)/2$ binary classifiers for detecting N number of classes. The performance parameters of the classifier, i.e cost-function C and kernel argument parameter γ are tuned using the particle swarm optimization (PSO) technique. The runtime complexity of kernel methods using an RBF kernel is '$O(n_{SV} \times d)$' where 'n_{SV}' is the number of support vectors and "d" is the input dimensionality. The PSO determines the best parameters to achieve maximum classification accuracy. The theory of PSO is briefly discussed in the next subsection.

3.3. Particle swarm optimization

Particle swarm optimization technique is a stochastic optimization technique based on social interaction of bird flocks introduced by Kennedy and Eberhart [27]. In PSO, the particles are placed in the search space of some problem or function to evaluate the objective function of its current location. The movement of each particle is determined by the past of its best (best-fitness) and current locations with the members of the swarm. The position and velocity of each particle are adjusted with previous best position and neighboring particle in the swarm. The PSO algorithm is briefly described here.

Each particle $P_i (i = 1, 2, \cdots, S)$ in the swarm of size S is represented by: 1) its position $\mathbf{x}_i(t) \in \Re^d$, which provide to a particle solution of the given problem; 2) its velocity $v_i(t) \in \Re^d$; and 3) the best position $\mathbf{x}_{bi}(t) \in \Re^d$ determined throughout its previous trajectory. The best position of the moving particles in the swarm for all the trajectories is given by $x_g(t) \in \Re^d$. The movement of particles during the search can be given by

$$\mathbf{v}_i(t+1) = w\mathbf{v}_i(t) + c_1 r_1(t)(\mathbf{x}_{bi}(t) - \mathbf{x}_i(t)) + c_2 r_2(t)(\mathbf{x}_g(t) - \mathbf{x}_i(t)) \tag{5}$$

$$\mathbf{x}_i(t+1) = \mathbf{x}_i(t) + \mathbf{v}_i(t) \tag{6}$$

where $r_1(\cdot)$ and $r_2(\cdot)$ are uniform random variables that enable stochastic search of the algorithm. c_1 and c_2 are acceleration coefficients that regulate the velocities of the particle. These factors determine the influence of a particle by its previous best positions and other particles of the swarm. An inertia weight "w" coefficient is utilized to control the local and global exploration degree of the search in a swarm. The greater value of "w" allows superior global exploration while lesser value allows a fine search in the solution space. The velocity of each particle is determined by Eq. (5) while the position of the particle is updated using Eq. (6). The iterations are carried until the convergence is reached for the search. In PSO, let A be the number of initial particles and B the number of iterations to

reach the global optimum, the computational complexity is in the order of $O(AB)$ (from Ref. [27], p. 313).

Despite of several optimization techniques available, the PSO is used in this study due to the following advantages:

- It is a derivative-free algorithm unlike many conventional techniques.
- It has the flexibility of integration with other optimization techniques to form hybrid tools.
- It has less parameter to adjust unlike many other competing evolutionary techniques.
- It has the ability to escape local minima.
- It is easy to implement and program with basic mathematical and logic operations.
- It can handle objective functions with stochastic nature, like in the case of representing one of the optimization variables as random.
- It does not require a good initial solution to start its iteration process.

4. Proposed methodology

This section presents the theory of the techniques utilized and a thorough description of the procedure employed in this study. The proposed methodology consists of four stages, namely, pre-processing, R-peak detection, feature extraction, classification stages as depicted in Fig. 1. Initially, the raw cardiac signals are pre-processed to remove artifacts and consequently R-peak is detected using Pan–Tompkins algorithm [28]. The R-peak detection is followed by a window which extracts each cardiac signal segment. Thenafter, discrete orthogonal stockwell transform (DOST) is applied to extract the symmetrical morphological characteristics which are represented in lower dimensional space using principal component analysis (PCA). Additionally, the dynamic features are concatenated to the morphological features that are classified using support vector machine into different cardiac signal classes utilizing the category-based and patient-based assessment schemes. The parameters of the classifier are optimized using particle swarm optimization (PSO) to yield better classification performance.

4.1. *Pre-processing*

Usually, the pre-processing is done to increase the signal-to-noise ratio (SNR) and to eliminate various types of noise that are inherited inside the cardiac signals. The pre-processing step is highly instrumental for the subsequent fiducial point detection and classification of cardiac signal analysis. The types of noise that degrade the quality of ECG signals include artifacts due to muscle contraction, power-line interference, electrode movement and baseline wander. Therefore, a wavelet-based approach [29] followed by band-pass filter at 5–12 Hz [28] has been adopted to correct the baseline wander and maximizing the energy of QRS content. Thenafter, the filtered ECG signal is further processed for classifying the cardiac signals into their subsequent categories.

4.2. *R-peak detection and heartbeat segmentation*

For practical applications, it is necessary to detect the R-peak automatically to evaluate the proposed algorithm entirely for cardiac event diagnosis. The well known Pan and Tompkins algorithm [28] is employed here due to its proven sensitivity of 99.87% to detect the R-peak in the subsequent cardiac signals. Fig. 2 shows the plots of the various stages involved in the R-peak detection of the ECG signal using the Pan–Tompkins algorithm. In Fig. 2, record #100 from the MIT-BIH database is selected and passed through the subsequent stages, i.e. cascading of low pass and high pass filters, derivative, squaring, averaging and moving window integrator stages to detect the QRS complex in the cardiac signal.

It is provided that the sampling rate of database is 360 Hz. In this study, each heartbeat segment consists of 110 samples before the R peak location and 146 samples after the R peak corresponding to the pre-R segment and pro-R segment respectively, i.e. a total of 256 samples is selected to determine the length of each event corresponding to 0.712s window size. The length of fragments is selected to incorporate most of the information regarding each cardiac event. The detection of the R-peak is verified with the annotated file provided in the database.

The benefit of fixing the length of each cardiac event is to locate the R-peak accurately relative to P and T wave due to the fact that they have low amplitude and are noise sensitive. The aim of such segmentation remains to detect the more profound R-peaks.

4.3. *DOST based feature extraction and complexity analysis*

The complete architecture of the discrete orthogonal stockwell transform is presented in Fig. 3. Initially, the input ECG signal

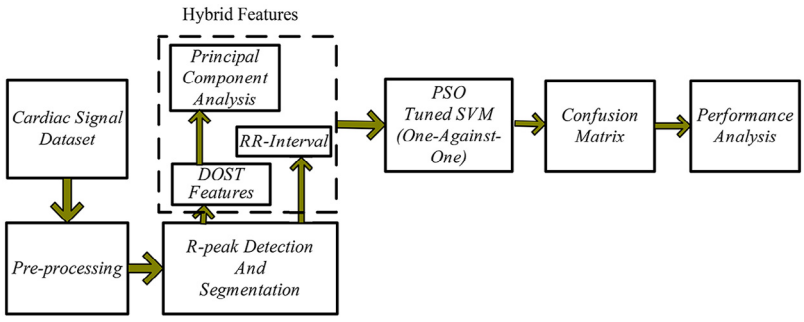

Fig. 1 – Block diagram of the proposed methodology.

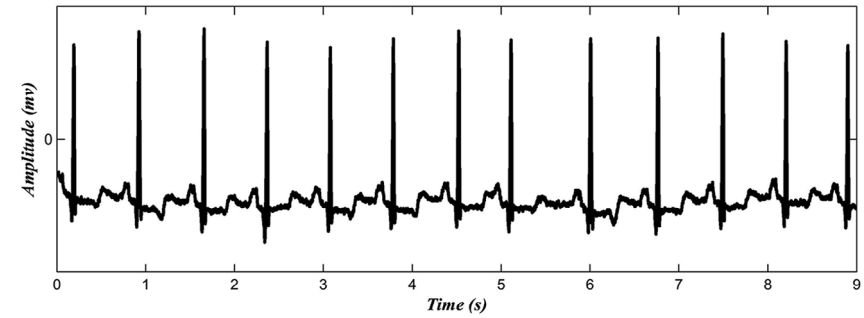

(a) Input ECG signal record #100

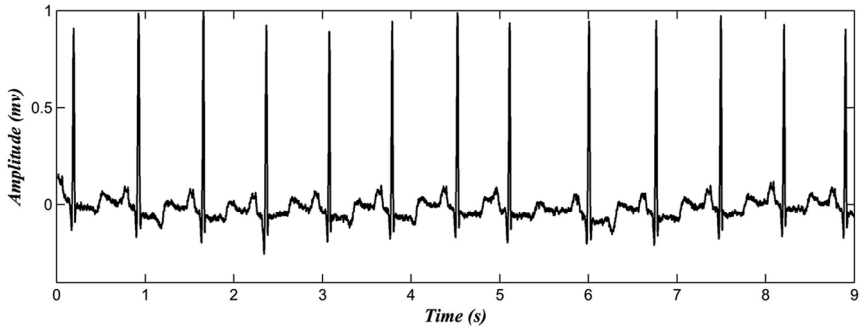

(b) ECG signal after removal of DC drift and normalization

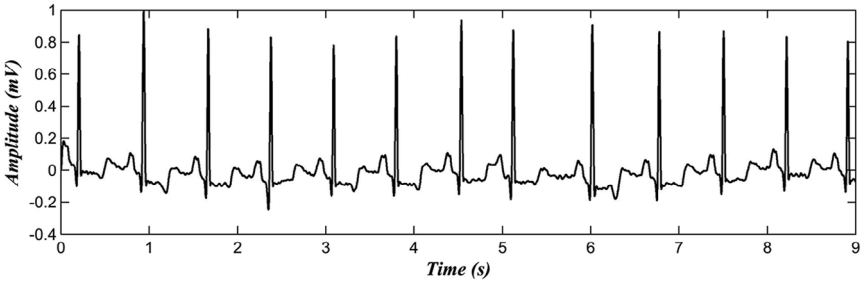

(c) ECG Signal after low-pass filter

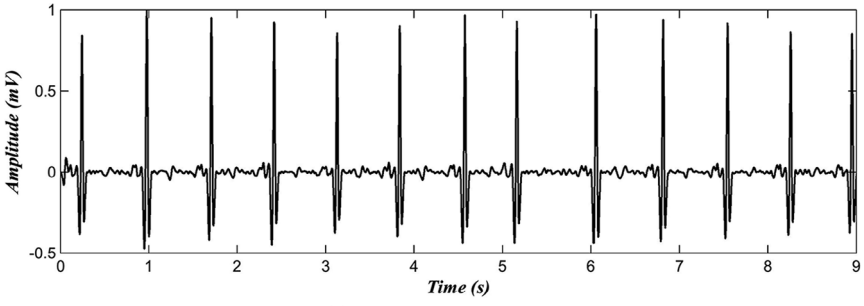

(d) ECG Signal after high-pass filter

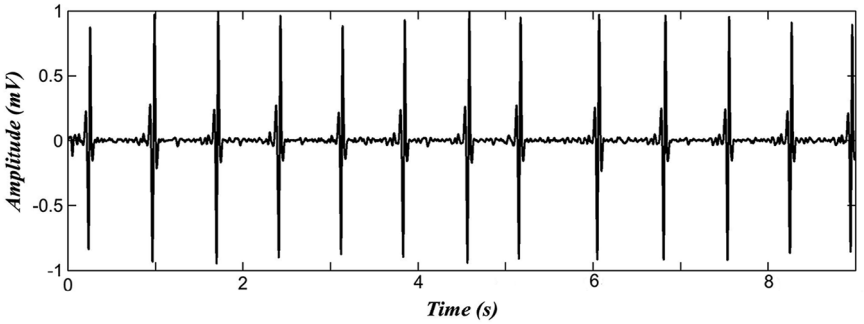

(e) ECG Signal after derivative stage

Fig. 2 – Different stages involved in Pan–Tompkins algorithm [28].

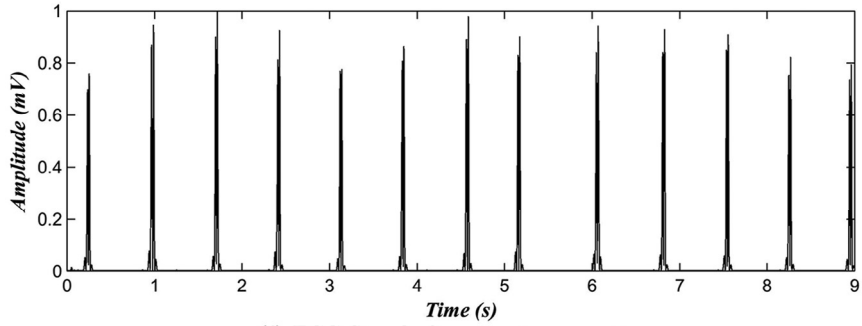

(f) ECG Signal after squaring operation

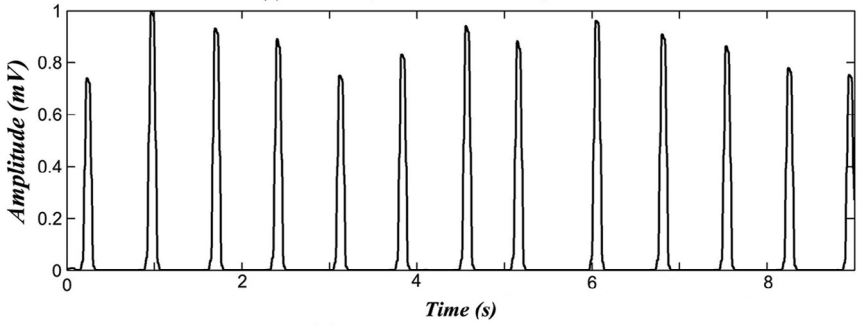

(g) ECG Signal after averaging

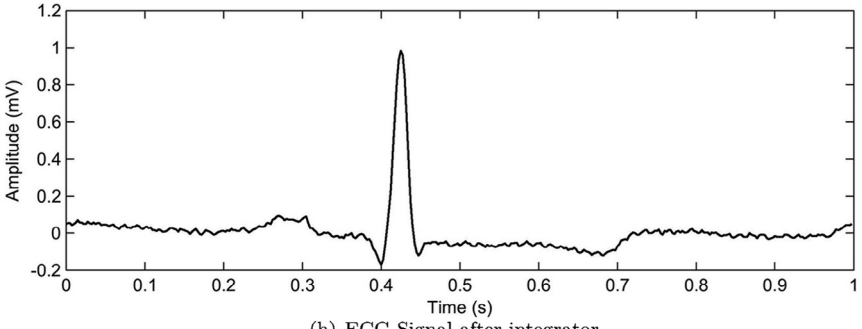

(h) ECG Signal after integrator

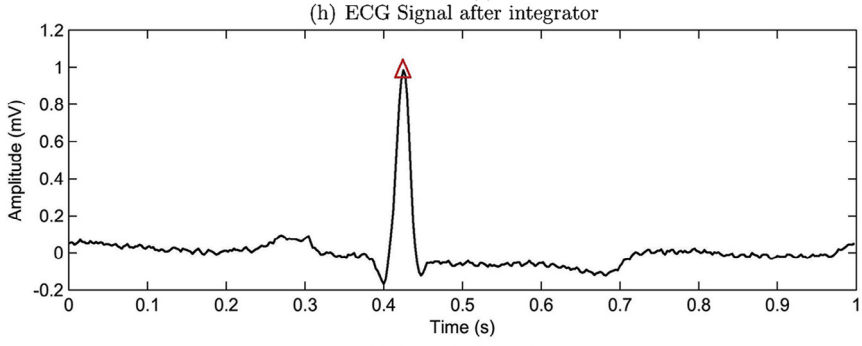

(i) R-peak detection

Fig. 2 – (*continued*)

is passed through the N-point FFT stage. This stage generates the FFT coefficients which are shown as $F_1, F_2, \cdots, F_N$. These coefficients obtained are partitioned into the sub-bands for the length as according $[2^0, 2^1, 2^2, \cdots, 2^{N-1}]$. However, in the block diagram the coefficients are partitioned for an input signal of length $N = 16$ (i.e. for space constraint) for representation. Across each sub-band, β-point inverse FFT is applied to obtain the final real coefficients that is localized in space. It is to note that β-point inverse-FFT is taken for computation of these coefficients that ensures the β are created in the frequencies and the decomposition is orthogonal. It is to note that here, β is the width of the frequency band, τ is the time variable indicating the time localization and ν is a frequency variable indicative of the center of a frequency band. These coefficients are re-arranged and considered as the morphological descriptor for each of the input ECG signals. The time-frequency order of coefficients for a morphological feature is shown in last as output where the values of coefficients are denoted as $A_1, A_2, \cdots, A_N$.

Fig. 4 shows the normalized frequency vs time plot of the symmetrical orthogonal coefficients. The darker the region in Fig. 4, the greater is the value of the coefficients and these

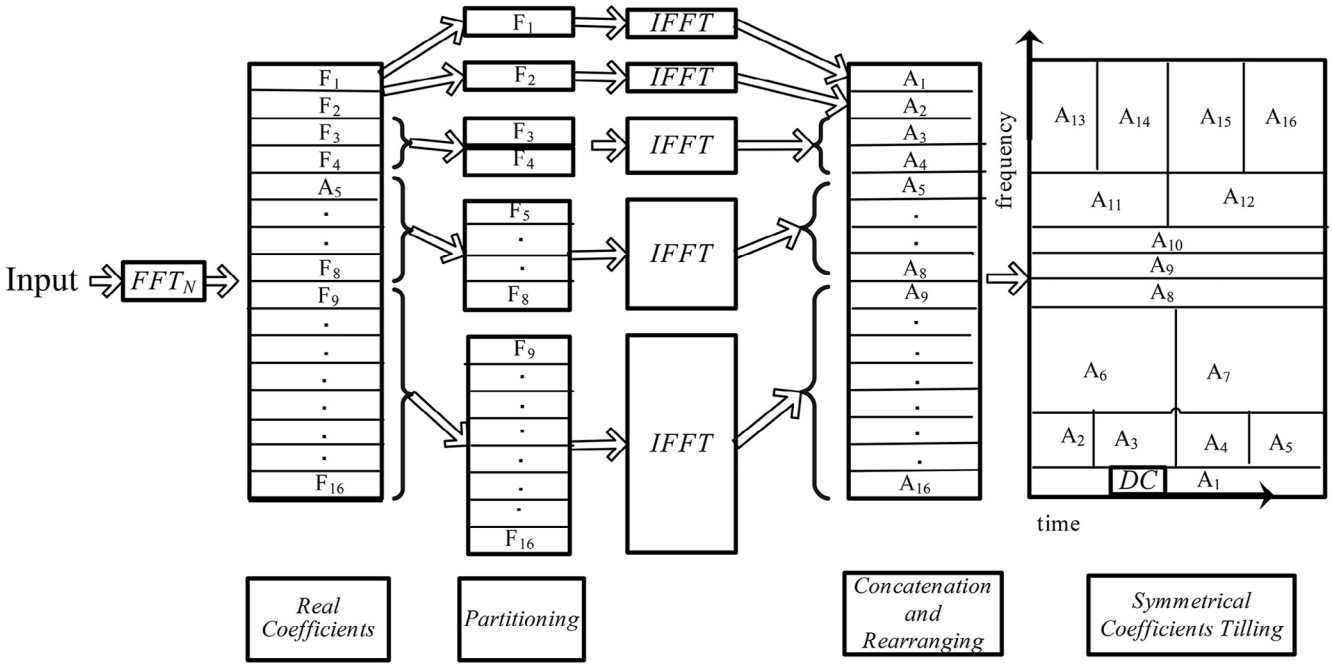

Fig. 3 – Architecture of the DOST algorithm.

values of the coefficients are uniformly distributed (i.e. as a result of octave sampling for N = 256 [1, 1, 2, 4, 8, 16, 32, 64, 64, 32, 16, 8, 4, 2, 1, 1] in the frequency band representing the positive frequencies in increasing order (from middle to top and negative frequencies in decreasing order from middle to bottom).

The complexity of DOST is also estimated here. The calculation of FFT of input signal *x* requires $\Theta NlogN$. Two power FFTs for calculating DOST coefficients will take less than $\Theta NlogN$. The remaining frequency band division steps and shuffling of DOST coefficients will take few ΘN. Hence, the total time complexity is of order $\Theta(NlogN)+(NlogN)+(N)$. IDOST involves the same steps in reverse order so it takes the same time in reverse order so its time complexity is of order $\Theta 2(NlogN)+N$.

4.4. *Principal component analysis (PCA)*

Two-hundred and fifty-six DOST coefficients, i.e [1 × 256] are computed and used to represent each of the cardiac event. Thenafter, PCA is applied to these DOST features to reduce the

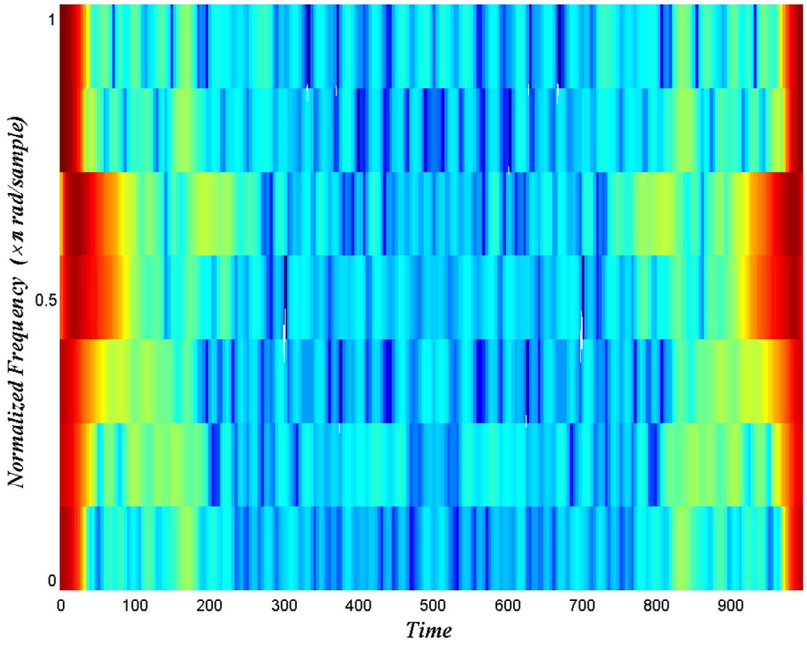

Fig. 4 – Normalized frequency vs time plot.

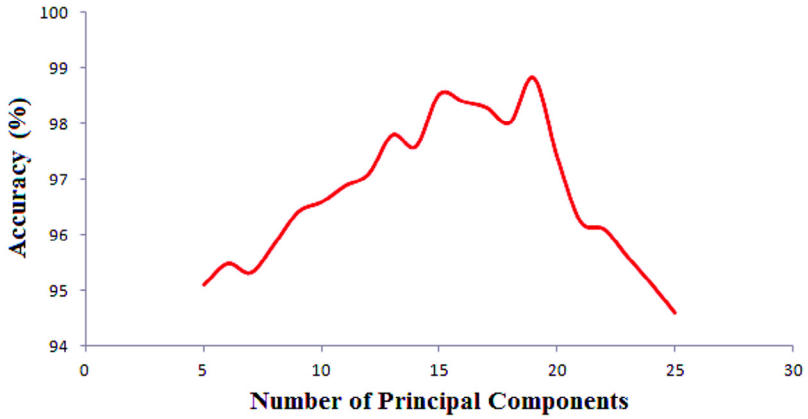

Fig. 5 – Variation in accuracy with the number of PCs.

feature dimensionality. In order to determine the optimal dimension of the PCs from the pre-defined training dataset as in Table 1, ten-fold cross validation is conducted. Nine beats are selected randomly for each class in each recording (all the beats are utilized if the count is less than nine) for training. In total, 976 beats including all the sixteen classes were utilized from the training dataset to estimate the optimal dimensionality of the PCs that are referred as morphological features. The trained PCs are applied to both the training and testing datasets. Fig. 5 shows the variation in the number of PCs on X-axis with the accuracies on Y-axis utilizing the pre-defined dataset. It can be concluded from this plot that nineteen features yielded the maximum classification accuracy above 98.5% and hence, are selected to represent each cardiac signal corresponding to variance of almost 90% in the training dataset.

The analysis of morphological descriptors (i.e. in the form of PCs) extracted from the various cardiac signals is carried out graphically in 3-dimensional (3-D) plot which is depicted in Fig. 6. Due to space constraint, in these plots the projection of PCs for Normal and APC beat features only are presented that corresponds to a particular combination of features (i.e. first three PCs) for the resulting morphological feature set (i.e. symmetrical + PCA) of cardiac signals. The reason behind the 3-dimensional plot for two classes only is to study the behavior of features for one-against-one classification approach utilized in this study. It is to note that the PCs computed for the subsequent signals carry energy in the decreasing order, i.e. the first PC contains the highest energy [30]. However, Fig. 6 illustrates that the features are decreasing values of the coefficients and not linearly separable, thereby overlapping with each other which can introduce ambiguity in the detection of cardiac signals which is overcome by employing kernel based SVM classifier for the detection of arrhythmias presented in the next subsection.

The morphological descriptors exhibit the characteristic inherited in the interior of the cardiac signals, whereas the dynamic features represent the characteristics between the consecutive ECG signals. The length of each morphological feature set is [1 × 256], while the length of each dynamic feature set is [1 × 4] (i.e. discussed in the next subsection). As such, in order

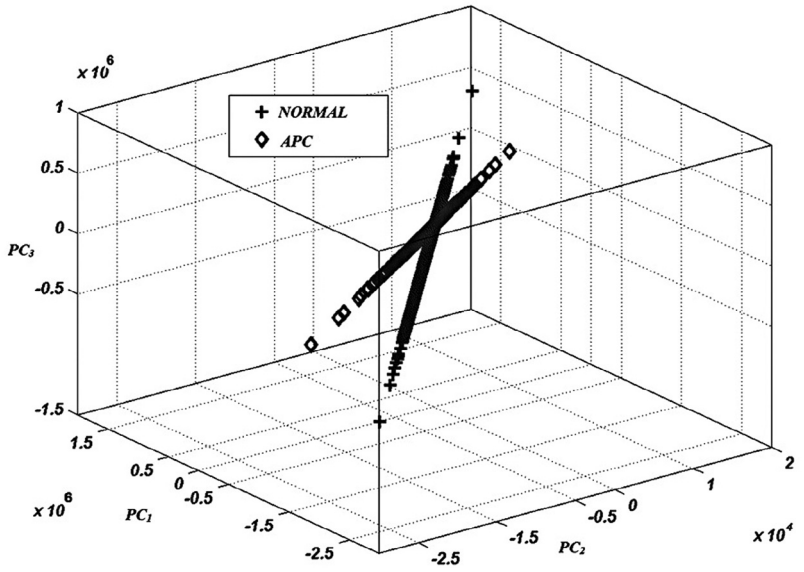

Fig. 6 – 3D plot of the normal and APC features.

to balance the characteristics of these two different kind of features, PCA is employed for morphological attributes only prior to their combination. Rather, an uneven amount of these features shall degrade the classifier performance.

4.5. *RR-interval features*

The RR-interval (dynamic) features are determined to realize the dynamic characteristic of the cardiac signals. Therefore, four RR features are computed which correspond to the pattern of cardiac signals, namely, pre-RR, post-RR, local-RR, and average-RR interval features.

The RR-interval features computed are different from Refs. [3,5] in which the feature appears to be similar for each cardiac event of a particular recording. This kind of the local and average RR feature is not practical for real-time applications and could be partial for the dynamic feature analysis. In this study, the interval between a previous R-peak and the current R-peak is computed to determine the pre-RR feature. While the interval between a given R-peak and the followed R-peak is computed to determine the post-RR feature. The combination of the pre and post RR-interval feature of the cardiac signals corresponds to an instantaneous rhythm characteristic. The average RR interval feature is derived by averaging the RR intervals of the past 3-min episode of a particular event. Likewise, the local-RR feature is derived by averaging all the RR-intervals of the past 8-s episode of a particular event. These both represent the average characteristics of a series of cardiac signals.

Finally, these four dynamic features are concatenated with the morphological descriptor of the ECG beats. As a result, twenty-three features (i.e. four RR-interval features and nineteen PCs features) are determined to represent each heartbeat. Further, these combined features are applied to support vector machines for classification.

4.6. *Proposed SVM-PSO model*

The challenge of parameter selection, i.e. "C" and "σ" in SVM concerns the problem of determining the function that can provide the best generalization capability to correctly classify patterns. In this study, PSO finds the optimum values of performance parameter, i.e. "C" and "σ" for the SVM classifier. The selection of the best parameters for SVM-RBF using PSO is performed offline, although the choice of the kernel function parameter is purely data dependent and selected empirically. The radial basis function (RBF) kernel is utilized for implementing the SVM approach in this study for the classification of ECG signals. The RBF kernel is represented by the equation as $(K(x_i, x_j) = exp^{-\gamma\|x_i - x_j\|^2})$. The regularization parameter C and kernel function argument parameter γ are varied in the range of $[10^{-3}, 50]$ and $[10^{-3}, 2]$ chosen randomly and are optimized using PSO technique. In the classification phase one-against-one approach is adopted in order to address the multi-class analysis scheme.

The PSO aims is to select the best optimal parameters for the SVM classifier. The PSO algorithm is summarized as follows:

1) A swarm of size S is initialized.
2) The velocity $v_i (i = 1, 2, \cdots, S)$ of the S particles in the swarm are set to zero.

Table 3 – Parameters utilized in the PSO approach.

Inertia weight (w)	0.7
Swarm size (S)	40
Acceleration constants ($c_1 and c_2$)	1.2
Range of velocity	$V_{max} = -V_{min} = X_{max}/2$
Position parameters	$X_{max} = -X_{min} = 0.2$

3) The SVM classifier is trained for each position $x_i \in \Re^{d+2}$ of the particle $P_i (i = 1, 2, \cdots, S)$ in the swarm and corresponding fitness function $f(i)$ is calculated.
4) The best position is set with the initial position of each particle as

$$\mathbf{x}_{bi} = \mathbf{x}_i, (i = 1, 2, \cdots, S) \tag{7}$$

5) The best global position x_g in the swarm is detected which corresponds to the lower value of the fitness function considered for all trajectories.
6) The velocity of each particle is updated using Eq. (5).
7) The position of each particle is updated using Eq. (6). The update is stopped if a particle travels beyond the predefined boundaries of the search space. This is done by fixing the position of the particle and by reversing the direction of search. This will not allow the particle to travel beyond the search space.
8) The SVM classifier is trained and the corresponding fitness function $f(i)$ is computed for each particle $p_i (i = 1, 2, \cdots, S)$.
9) If the current position $x_i (i = 1, 2, \cdots, S)$ of each particle has a lower fitness function then its best position x_{bi} is updated.
10) Goto step 5, if maximum iterations is not achieved.
11) The best global position x_g^* is selected in the swarm and the SVM classifier is trained with the features mapped by x_g^* and modeled with the values of cost function and kernel parameters at the same position.
12) The ECG signals are tested with the trained SVM classifier.

In this study, analysis for sixteen classes of cardiac signal is performed as $\Omega = w_1, w_2, \cdots, w_{16}$ and hence sixteen binary SVM models are optimized using the PSO technique. The utilization of PSO will automatically determine the best optimal parameters values of C and γ for each binary classifier.

In the PSO algorithm, the parameters utilized are summarized in Table 3. PSO evaluates the fitness of each particle at each iteration for a specific set of particles and finds the optimal network. The leave-one-out error bound is estimated using the class of criteria that reveals the unbiased performance of the classifier. Particularly, several measures of the error bound is presented in literature such as SV count [31] and the radius–margin bound. In this study, the simple SV count is explored as a fitness criterion in the PSO optimization network because it is simple and effective. The parameters C and γ are gradually tuned with the PSO algorithm in the training phase. During the training phase, the SVM parameters are selected according to a m-fold cross-validation strategy [32]. The ten-fold cross-validation is performed on the training dataset using the predefined values of C and γ. The best optimized parameters

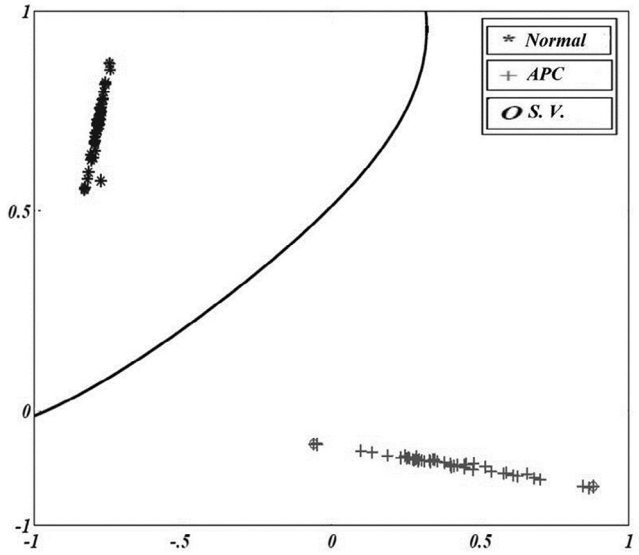

Fig. 7 – Hyperplane separating the normal and APC features.

for the SVM classifier are chosen to yield maximum classification performance. In the 10-fold cross-validation strategy, i.e the datasets are split into 10 different folds or test sets. The model is trained using the training dataset and tested using the first fold to get a confusion matrix. This confusion matrix represents the classification of 1/10 of the data. Further, the confusion matrix is computed for all the rest of the nine folds. The overall performance of the classifier is evaluated by taking the average of all the ten folds.

Fig. 7 shows a distinct separation between the overlapping hybrid features of Normal and APC classes into two regions using the best parameters optimized by PSO for RBF kernel through the resulting decision hyperplane. Fifty features are selected for both the classes to illustrate this figure. The testing is performed for each category of the testing dataset while the classification performance for each class of ECG signal is presented in the form of confusion matrix.

4.7. *Performance evaluation*

The performance analysis for each class of event is estimated by computing True Positive (T_P), False Positive (F_P) and False Negative (F_N) parameters, where (T_P) represents the correct classification of the normal ECG patterns. F_N represents the misclassification of normal as abnormal beats while F_P represents the misclassification of the abnormal beats into normal beats. On the basis of these T_P, F_P, F_N parameters, the performance metrics for each class of beat are calculated namely sensitivity and positive predictivity where sensitivity is the rate of correctly classified signals among the total number of signals given by $(S_e) = \frac{TP}{TP+FN} \times 100$. Whereas positive predictivity refers to the rate of correctly classified signals in all detected signals given by $(P_p) = \frac{TP}{TP+FP} \times 100$.

$$Sensitivity(S_e) = \frac{TP}{TP+FN} \times 100 \quad (8a)$$

$$PositivePredictivity(P_p) = \frac{TP}{TP+FP} \times 100 \quad (8b)$$

The overall accuracy and error rate is given by:

$$(\%)\text{Classifier Accuracy} = \frac{\text{Total correctly classified beats}}{\text{Total number of Beats}} \times 100 \quad (9)$$

$$(\%)Error = \frac{\text{Total misclassified beats}}{\text{Total number of beats}} \times 100 \quad (10)$$

5. Results and discussion

The experiments using the proposed methodology as discussed in the earlier section are performed and implemented on the MATLAB software package with hardware configuration of Intel Core™ i5-processor CPU 3.30 GHz and 4.00 GB of RAM. The methodology is validated on the benchmark of the MIT-BIH arrhythmia database. The combination of dynamic and morphological features are trained on the training dataset using the lead A signals and tested under evaluated under two assessment schemes described in Section 2. The SVM classifier performed is presented at convergence during the optimization procedure using PSO. The time taken for tuning the model parameters of SVM with the training data by PSO is approximately 2496.97s with the aforesaid configuration. It is to note that in PSO, the dimension of each particle defined by its velocity and position vectors in the swarm is 258. The trained classifier predicts the class of each tested cardiac signal into sixteen classes in the category-based and five classes in the patient-based assessment scheme. The time of execution using tuned SVM-RBF classifier by PSO in the testing phase is 3243.65s, while the output of each class of signal is presented in the form of confusion matrix and provided in Table 4 for detailed analysis.

In Table 4, each column corresponds to the number of ECG beats detected by the proposed methodology while each row corresponds to the actual number of signals annotated (i.e ground truth) at the database. The confusion matrix is described here for the LBBB class of signal for better understanding of readers. In Table 4, the row 2 belongs to the LBBB category and reports 5211 LBBB signals are correctly classified out of 5247 LBBB signals. However, the difference of the signals is misclassified into the different categories. While column 2 reports that 5275 signals are classified as LBBB signals where 64 signals in total belong to other categories. In total, a total of 84,805 signals are correctly classified out of 86,113 tested beats representing an accuracy of 99.18% and error rate of 0.82% for the proposed methodology is achieved in the category-based scheme. The symmetrical features alone contributed to achieve a classification accuracy of 98.26%, while the combination of symmetrical features with PCA reported a classification accuracy of 98.83% respectively. The combination of the RR-features to the feature set yielded in an improved classification

Table 4 – Confusion matrix in category-based scheme.

		Correctly classified instances: 85,407																
		Misclassified instances: 706																Accuracy: 99.18%
		Ground truth																Error rate: 0.82%
	Class	N	L	R	A	V	P	a	!	F	x	j	f	E	J	e	Q	Total
Predicated	N	63345	13	0	187	95	0	18	23	37	0	29	9	0	0	5	3	63,764
	L	14	5224	0	0	9	0	0	0	0	0	0	0	0	0	0	0	5247
	R	23	0	4657	19	8	0	0	0	0	0	0	0	0	9	0	0	4716
	A	8	3	0	1624	6	0	0	5	9	0	0	0	0	0	0	0	1655
	V	15	7	0	0	4591	0	0	8	11	0	0	2	0	0	0	0	4634
	P	0	29	0	0	0	4515	0	0	0	0	0	22	0	0	0	0	4566
	a	2	0	0	1	3	0	69	0	0	0	0	0	0	0	0	0	75
	!	0	13	0	0	8	0	0	215	0	0	0	0	0	0	0	0	236
	F	11	0	0	0	2	0	0	0	387	0	0	0	0	1	0	0	401
Labels	x	3	0	0	2	0	0	0	1	0	90	0	0	0	0	0	0	96
	j	1	0	0	0	0	0	0	0	0	0	112	0	0	1	0	0	114
	f	7	6	0	0	0	3	0	0	0	0	0	475	0	0	0	0	491
	E	0	0	0	0	0	0	0	0	0	0	0	0	53	0	0	0	53
	J	2	0	0	2	0	0	0	0	0	0	0	0	0	37	0	0	41
	e	3	0	0	0	0	0	0	0	0	0	0	0	0	0	5	0	8
	Q	4	0	0	0	1	0	0	0	0	0	0	3	0	0	0	8	16
	Total	63,438	5295	4657	1835	4723	4518	87	252	444	90	141	511	53	48	10	11	86,113

accuracy 99.18%. However, the accuracy of the SVM classifier (without PSO) yielded an accuracy of 97.62% and with PSO yielded 99.18%. It is to note that the performance parameters of the SVM classifier alone (i.e. the parameters are not tuned using PSO technique) are selected empirically, i.e. based on trial and error. It can be concluded that the utilization of PSO reported an improved classification accuracy where the symmetrical features contributed the most. Thenafter, performance analysis for each class of the cardiac signal employing the proposed methodology is computed and presented in Table 5.

The performance parameters, i.e TP, FP, FN for each class of cardiac signal are computed and presented in Table 5. On the basis of these parameters, the sensitivity and positive predictivity evaluation parameters are analyzed for detailed study. From Table 5, it can be concluded that the unclassificable beat (UN) reported a very low sensitivity of 50% and positive predictivity of 72.73%. While ventricular escape (VE) beat reported the maximum sensitivity and positive predictivity of 100%. A brief comparison of number of cardiac signals classified and the classification accuracy between the proposed methodology and earlier reported works [8,19,20,33–35] in the category based assessment scheme is presented in Table 6. To have such comparison is quite tedious because it depends on several factors like the database used, number of cardiac beats considered for training and testing datasets, and the number and class of beats identified. Several works also involve the data taken from the hospitals or patients. Taking account of these factors, works performed on MIT-BIH arrhythmia database is presented in this study. It is to note that the "category-based"

Table 5 – Performance assessment of each class of cardiac signal in category based scheme.

Heartbeat class	Trained beats	Test beats	FN	TP	FP	S_e (%)	P_p (%)
N	11,253	63,764	419	63,345	93	99.34	99.85
L	2825	5247	23	5224	71	99.56	98.66
R	2539	4716	59	4657	0	98.75	100
A	891	1655	31	1624	211	98.13	88.50
V	2495	4634	43	4591	132	99.07	97.21
P	2458	4566	51	4515	3	98.89	99.93
a	75	75	6	69	18	92	79.31
!	236	236	21	215	37	91.10	85.32
F	401	401	14	387	57	96.51	87.16
x	97	96	6	90	0	93.75	100
j	115	114	2	112	29	98.25	79.43
f	491	‘491	16	475	36	96.74	92.95
E	53	53	0	53	0	100	100
J	42	41	4	37	11	90.24	77.09
e	8	8	3	5	5	62.5	50
Q	17	16	8	16	3	50	72.73
Total	23,996	86,113	706	85,407	706	99.18	99.18

TP corresponds to True Positive, TN corresponds to True Negative, FP corresponds False Positive.

Table 6 – Comparison with existing methodologies for category-based assessment scheme.

Literature	Techniques	Classes	Accuracy (%)
Osowski [8]	HOS + Hermite	13	98.18
Qiao et. al [19]	Features + SVM	5	98.60
Rodriguez [33]	Morphology + decision	16	96.13
Lagerholm [34]	Hermite + SOM	16	98.49
Prasad [35]	Wavelet + RR	13	96.77
Martis et. al [20]	PCA + SVM	5	93.48
Fatin et. al [15]	WT + PCA	5	98.91
Dokur et. al [36]	WT + MLP-NN + GA	10	96
Proposed	DOST + SVM-PSO	16	99.18

SOM: self-organizing map, BPNN: back propagation neural network, LS-SVM: least square support vector machines, PCA: principal component analysis, WT: wavelet transform, MLP-NN: multi layer perceptron neural network, GA: genetic algorithm.

assessment of the classifier performance is not practical and feasible for real applications. As such, it provides a measure of the capability of the proposed method to detect a particular event when they are perfectly modeled. This assessment is done to make a comparison with previous reported works in Refs. [8,19,20,33–35]. It can be concluded that the proposed approach provides improvement in cardiac event classification accuracy over the reported works in literature with more number cardiac signals classified in the category-based assessment scheme. The results reported for the proposed methodology based on DOST features can be understood as a measure of performance if the classifier is trained using the data of patients under study.

In the patient-based assessment scheme, the classification performance following the ANSI/AAMI standard for five-classes utilizing 22 records for training and testing datasets, as in Refs, [3,16,37] is presented in Table 7, while the classification performance in the form of confusion matrix for cross-validation approach performed on the 44 folds to determine the category from a particular record trained on 43 folds is calculated by averaging the accuracies and presented in Table 8. The confusion matrices of the two above mentioned tests for the proposed feature set are shown in Tables 7 and 8 respectively. The results reported are compared with the results in Refs. [3,37] depending upon the following performance parameters, namely, classification accuracy, S_e and $+P$. The comparison of the patient-based assessment scheme with the existing works in literature is presented in Table 9.

It can be observed from Table 9 that the proposed method yielded comparable performances in terms of classification accuracy and the performance parameters. The performance of the class "S" is worse, which may be due to lesser number of training data for class "S" than class "V". The degraded performance of the "patient-based" assessment scheme was expected than that of the "category-based" assessment scheme due to variation in the characteristics of same morphologies of different patients. However, the improved classification accuracy suggests that the proposed feature representation of cardiac signals, based on the combination of symmetrical and dynamic features, exhibits superior performance for distinguishing a particular cardiac signal from various other classes of signals in both the assessment schemes in comparison with the existing methodologies presented in literature.

Table 7 – Confusion matrix under patient-based .

		Predicted label					
	Class	n	s	v	f	q	TN
Reference	N	39,513	887	1141	2658	39	4725
	S	486	1259	211	9	7	713
	V	203	121	2817	71	8	403
	F	177	2	137	69	3	251
	Q	2	0	4	0	1	6

Table 8 – Confusion matrix of cross-validation under patient-based scheme.

		Predicted label					
	Class	n	s	v	f	q	TN
Reference	N	81,533	1039	3453	3987	71	8550
	S	643	1893	437	21	9	1079
	V	403	178	6574	297	26	906
	F	346	3	145	304	4	498
	Q	4	3	6	1	1	14

6. Conclusion

In this article, symmetrical morphological features are extracted in time–frequency space using DOST that retains the absolute phase information which is brought in lower dimensional space using PCA and combined with the dynamic features, i.e RR-interval features. Finally, the classification is performed using twenty-three projection coefficients representing the feature set for each cardiac signal. This feature set is utilized in the classification of sixteen cardiac event classes using PSO tuned SVMs. The proposed feature representation of cardiac signals based on symmetrical features yields an improved accuracy of 99.18% in the category-based and 89.10% in the patient-based assessment schemes evaluated on the benchmark MIT-BIH arrhythmia database. The future scope of this work is to increase the number of detectable cardiac signals and the implementation of the proposed methodology on a suitable hardware platform. These platforms can provide an automatic diagnostic solution in the domain of health care.

Table 9 – Comparison with existing methodologies under patient-based assessment scheme.

Metric	Ye [10]	De Chazal [3]	Proposed	Proposed[a]
Accuracy (%)	86.4	81.9	87.62	89.10
S_e (%) of Class "S"	60.8	75.9	63.84	63.4
$+P$ (%) of Class "S"	52.3	38.5	55.49	60.75
S_e (%) of Class "V"	81.5	77.7	87.48	87.91
$+P$ (%) of Class "V"	63.1	81.9	65.36	61.93

[a] represents the cross-validation approach.

Acknowledgment

We acknowledge the Department of Science and Technology (IF 120841), Government of India for sponsoring this research work under DST-INSPIRE Fellowship Scheme.

REFERENCES

[1] World Health Organization, Global status report on noncommunicable diseases, 2014, available at: http://www.who.int/mediacentre/factsheets/fs317/en/.
[2] E. José da S. Luz, W.R. Schwartz, G. Cámara-Cháveza, D. Menotti, ECG-based heartbeat classification for arrhythmia detection: a survey, Comput. Methods Programs Biomed., 127, (2016), pp. 144–164. http://dx.doi.org/10.1016/j.cmpb.2015.12.008.
[3] P. de Chazal, M.O. Dwyer, R.B. Reilly, Automatic classification of heartbeats using ECG morphology and heartbeat interval features, IEEE Trans. Biomed. Eng., 51 (7), (2004), pp. 1196–1206.
[4] Y. Hu, W. Tomkins, J.L. Urrusti, V.X. Afonso, Application of artificial neural networks for ECG signal detection and classification, J. Electrocardiol., 26, (1993), pp. 66–73.
[5] F.D. Chazal, R.B. Reilly, A patient adapting heart beat classifier using ECG morphology and heartbeat interval features, IEEE Trans. Biomed. Eng., 53 (12), (2006), pp. 2535–2543.
[6] S. Raj, K. Maurya, K.C. Ray, A knowledge-based real time embedded platform for arrhythmia beat classification, Springer, Biomed. Eng. Lett., 5 (4), (2015), pp. 271–280. http://dx.doi.org/10.1109/TIM.2014.2317296.
[7] F. Melgani, Y. Bazi, Classification of electrocardiogram signals with support vector machines and particle swarm optimization, IEEE Trans. Inf. Tech. Biomed., 12 (5), (2008), pp. 667–677.
[8] S. Osowski, L.T. Hoai, T. Markiewicz, Support vector machine-based expert system for reliable heartbeat recognition, IEEE Trans. Biomed. Eng., 51 (4), (2004), pp. 582–589. http://dx.doi.org/10.1109/TBME.2004.824138.
[9] Y. Kutlua, D. Kuntalp, Feature extraction for ECG heartbeats using higher order statistics of WPD coefficients, Comput. Methods Programs Biomed., 105 (3), (2012), pp. 257–267. http://dx.doi.org/10.1016/j.cmpb.2011.10.002.
[10] C. Ye, B. Kumar, M. Coimbra, Heartbeat classification using morphological and dynamic features of ECG signals, IEEE Trans. Biomed. Eng., 59 (10), (2012), pp. 2930–2941. http://dx.doi.org/10.1109/TBME.2012.2213253.
[11] K. Minami, H. Nakajima, T. Toyoshima, Real-time discrimination of ventricular tachyarrhythmia with fourier-transform neural network, IEEE Trans. Biomed. Eng., 46 (2),(1999), pp. 179–185.
[12] S. Raj, S. Luthra, K.C. Ray, Development of handheld cardiac event monitoring system, 13th {IFAC} and {IEEE} Conf. on Programmable Devices and Embedded Systems PDES 2015, IFAC-Papers-OnLine, 48 (4) (2015), pp. 71–76. http://dx.doi.org/10.1016/j.ifacol.2015.07.010.
[13] T. Ince, S. Kiranyaz, M. Gabbouj, A generic and robust system for automated patient-specific classification of ECG signals, IEEE Trans. Biomed. Eng., 56 (5), (2009), pp. 1415–1426.
[14] S. Raj, G.S.S. Praveen Chand, K.C. Ray, Arm-based arrhythmia beat monitoring system, Microprocess. Microsy., 39 (7), (2015), pp. 504–511. http://dx.doi.org/10.1016/j.micpro.2015.07.013.
[15] F.A. Elhaj, N. Salima, A.R. Harris, T.T. Swee, T. Ahmeda, Arrhythmia recognition and classification using combined linear and nonlinear features of ECG signals, Comput. Methods Programs Biomed., 127, (2016), pp. 52–63.
[16] M. Llamedo, J. Martinez, Heartbeat classification using feature selection driven by database generalization criteria, IEEE Trans. Instrum. Meas., 58 (3), (2011), pp. 616–625. http://dx.doi.org/10.1109/TBME.2010.2068048.
[17] W. Jiang, S. Kong, Block-based neural networks for personalized ECG signal classification, IEEE Trans. Neural Netw., 18 (6) (2007), pp. 1750–1761. http://dx.doi.org/10.1109/TNN.2007.900239.
[18] T. Linh, S. Osowski, M. Stodolski, On-line heart beat recognition using hermite polynomials and neuro-fuzzy network, IEEE Trans. Instrum. Meas., 52 (4), (2003), pp. 1224–1231. http://dx.doi.org/10.1109/TIM.2003.816841.
[19] L. Qiao, C. Rajagopalan, G.D. Clifford, A machine learning approach to multi-level ECG signal quality classification, Comput. Methods Programs Biomed., 117 (3), (2014), pp. 435–447.
[20] R. Martis, U. Acharya, K. Mandana, A. Ray, C. Chakraborty, Cardiac decision making using high order spectra, Biomed. Signal Process. Control, 8 (2), 2013, pp. 193–203.
[21] S. Raj, K.C. Ray, A comparative study of multivariate approach with neural networks and support vector machines for arrhythmia classification, IEEE Int. Conf. Energy, Power and Environment: Towards Sustainable Growth (ICEPE), Jun. 2015, pp. 1–6.
[22] R.G. Stockwell, L. Mansinha, R.P. Lowe, Localization of the complex spectrum: the S transform, IEEE Trans. Signal Process., 44 (4), 1996, pp. 998–1001.
[23] R.G. Stockwell, L. Mansinha, R.P. Lowe, A basis for efficient representation of the S-transform, Digit. Signal Process., 17 (1), 2006, pp. 371–393.
[24] G.B. Moody, R.G. Mark, The impact of MIT-BIH arrhythmia database, IEEE Trans. Biomed. Eng., 20 (3), (2001), pp. 45–50.
[25] O. Inan, L. Giovangrandi, G. Kovacs, Robust neural-network-based classification of premature ventricular contractions using wavelet transform and timing interval features, IEEE Trans. Biomed. Eng., 53 (12), (2006), pp. 2507–2515. http://dx.doi.org/10.1109/TBME.2006.880879.
[26] Testing and Reporting Performance Results of Cardiac Rhythm and ST Segment Measurement Algorithms, ANSI/AAMI EC57:1998 standard, Association for the Advancement of Medical Instrumentation, 1998.
[27] J. Kennedy, R.C. Eberhart, Swarm Intelligence, San Mateo, CA: Morgan Kaufmann 2001.
[28] J. Pan, W.J. Tompkins, A. Real-Time QRS detection algorithm, IEEE Trans. Biomed. Eng., BME-32 (3), (1985), pp. 230–236.
[29] A. Rabee, I. Barhumi, Ecg signal classification using support vector machine based on wavelet multiresolution analysis, in: Information Science, Signal Processing and their Applications (ISSPA), 2012 11th Int. Conf., 2012, pp. 1319–1323. http://dx.doi.org/10.1109/ISSPA.2012.6310497.
[30] B. Acar, H. Koymen, SVD-based on-line exercise ECG signal orthogonalization, IEEE Trans. Biomed. Eng., 46 (3), (1999), pp. 311–321. http://dx.doi.org/10.1109/10.748984.
[31] V. Vapnik, Statistical Learning Theory, New York: Wiley 1998.
[32] M. Stone, Cross-validatory choice and assessment of statistical predictions, J. R. Stat. Soc. [Ser B], 36. 1974
[33] J. Rodriguez, A. Goñi, A. Illarramendi, Real-time classification of ECGs on a PDA, IEEE Trans. Inf. Technol. Biomed., 9 (1), (2005), pp. 23–34. http://dx.doi.org/10.1109/TITB.2004.838369.
[34] M. Lagerholm, C. Peterson, G. Braccini, L. Edenbrandt, L. Sornmo, Clustering ECG complexes using hermite functions and self-organizing maps, IEEE Trans. Biomed. Eng., 47 (7), (2000), pp. 838–848. http://dx.doi.org/10.1109/10.846677.

[35] G. Prasad, J. Sahambi, Classification of ECG arrhythmias using multi-resolution analysis and neural networks, in: TENCON 2003. Conference on Convergent Technologies for the Asia-Pacific Region, Vol. 1, 2003, pp. 227–231, vol. 1. http://dx.doi.org/10.1109/TENCON.2003.1273320.

[36] Z. Dokur, T. Ölmez, ECG beat classification by a novel hybrid neural network, Comput. Methods Programs Biomed., 66 (2–3), (2001), pp. 167–181. http://dx.doi.org/10.1016/S0169-2607(00)00133-4.

[37] G. de Lannoy, D. Francois, J. Delbeke, M. Verleysen, Weighted conditional random fields for supervised interpatient heartbeat classification, IEEE Trans. Biomed. Eng., 59 (1), (2012), pp. 241–247. http://dx.doi.org/10.1109/TBME.2011.2171037.